Proceedings of the ASME 2011 International Mechanical Engineering Congress & Exposition
IMECE2011
November 11-17, 2011, Denver, Colorado, USA

IMECE2011-64108

AN ADMITTANCE TYPE HAPTIC DEVICE – RML GLOVE

Zhou MA
Robotics and Mechatronics Lab
George Washington University
Washington, DC, USA
mazhou@gwmail.gwu.edu

Pinhas Ben-Tzvi
Robotics and Mechatronics Lab
George Washington University
Washington, DC, USA
bentzvi@gwu.edu

ABSTRACT

This paper presents the design and control of a newly developed five-fingered admittance haptic interface named RML-glove. This haptic device is a lightweight and portable actuator system that fits on a hand and adds a sense of touch to each finger of the user. With this system, the operator is able to feel the shape and size of virtual 3D objects or to control robots through force feedback. Each finger has a miniature linear actuator that can be individually controlled to provide the force feedback. An embedded lead screw mechanism makes it possible to provide force feedback from almost zero and up to 40 N to each finger. The interface consists of micro-motors, force sensitive sensors, lithium-ion battery, wireless RF module, and an ARM7 micro-controller board. Wireless communication with a robot or host PC is established via unlicensed bands of 2.4 GHz. This haptic device may be worn on the back of bare hand without any other intrusive hardware, which otherwise constrain the movement of the fingers.

INTRODUCTION

The haptic interfaces discussed in this paper pertain to the sense of touch they can provide and used for bidirectional human–computer interaction (HCI). Haptic devices can measure the movement/force of the operators, and at the same time they can provide the operators with force/torque information from remote environments or virtual reality (VR). Recently, haptic devices have received extensive attention. They have been utilized in the areas of medical training and evaluation [1-3], rehabilitation, telesurgery, telemanipulation [4-7], telenavigation [8], as well as micromanipulation [9, 10].

During the last decade, several haptic devices with multiple finger inputs were developed [11-16]. These devices mainly can be divided into two categories: grounded and the exoskeleton types.

Grounded haptic devices mainly measure force at one point using instruments such as a pen or a ball. The operator can feel the feedback force from a wall and the weight of grasping an object. Therefore, the operator can manipulate the device with ease. However, there lies a fundamental problem in which the workspace becomes limited since the device is grounded and with this approach it is difficult to develop devices with multiple finger inputs. Another issue is that they are not capable of high force and torque output, although these devices are widely used in haptic display applications, such as computer games and medical simulations.

There are mainly two types of exoskeleton haptic devices. One of them is the CyberGrasp exoskeleton [17]. Most conventional exoskeleton type devices tend to be bulky and require an operator wearing a glove to measure the state of an operator's finger. The other one is the endoskeleton type such as Rutgers Master II [18]. Although it is light-weight and compact and does not require a glove, it does not allow complete fist closure due to the placement of the actuators in the palm.

Exoskeleton type haptic devices are mainly shaped like a glove to fit into the back of the hand. Since the shape of the device is very much like a hand, the operator can manipulate it intuitively. This type is more suitable for multiple finger inputs and has a larger workspace compared to the grounded type because the structure

is worn on the operator's hand. However, the operator has to bear the weight of the device and the device cannot display the weight of a grasping object or provide feedback force from a wall when in contact.

In summary, it has been demonstrated that both types of haptic devices have problems. To solve these problems, it is necessary to develop a new type of haptic device that accounts for the pros and cons of both types, while maintaining simplicity of design, compact structure, usability and comfort.

One major challenge in haptic sensations is that the human operator's motion should be unrestricted when there is no contact with a virtual or remote object. Haptic devices must allow the human operator to make desired motions, thus requiring back-drivability and sufficient degrees of freedom of motion. The size and shape of human fingers may vary significantly between individuals; to avoid custom design for each person, it is desirable to accommodate a large number of different people for a given design.

The proposed newly designed haptic device will attempt to solve all of the aforementioned issues. This RML-glove could present users with a real feel of grasp, applicable to all segments of each finger, as shown in Fig.1. The RML-Glove haptic device has the potential of being hand-holdable in an actual position in the operator's hand. It's also expected to be relatively lightweight. The design incorporates a multi-link redundant serial mechanism for each finger, in order to accommodate most hand sizes.

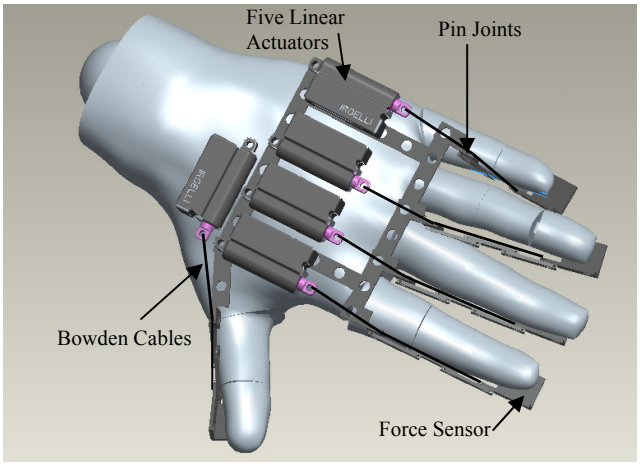

Fig. 1: CAD Model of RML-Glove

HUMAN HAND CAD MODEL

Before the design details are presented, the following sections discuss the kinematics simplification of the index finger as well as the development of a CAD hand model for the purpose of design development and simulations.

Kinematics simplification of the index finger

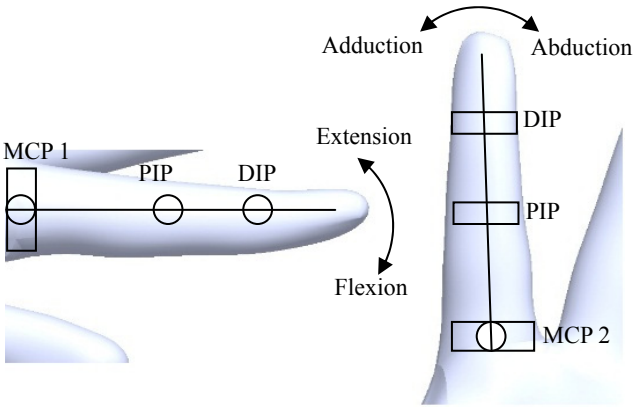

Fig. 2: Biomechanical Model of the Index Finger

The index finger can be modeled as a four-linkage mechanism with 4 DOFs, as shown in Fig. 2. There are 3 joints in total, which are referred to as DIP (distal interphalangeal), PIP (proximal interphalangeal), and MCP (metacarpophalangeal) joints. The MCP joint has 2 DOFs, which is divided into MCP1 and MCP2. This joint realizes movement of extension/flexion and adduction/abduction, respectively, while each of the DIP and PIP joints have only 1 DOF for extension/flexion.

For the purposes of the design and simulation, a hand CAD model with 20 DOF's was rendered, as shown in Figure 3. The MCP joints were implemented as ball joint connections, while the DIP and PIP were implemented as revolute joints.

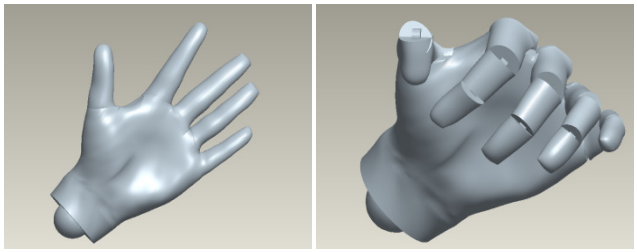

Fig. 3: Original and Assembled Hand Models

Index Finger Workspace

One major challenge in artificially generating haptic sensations is that the human operator's motion should be unrestricted when there is no contact with a virtual or remote object. Moreover, haptic devices must allow the human operator to make desired motions, thus requiring back-drivability and sufficient degrees of freedom of motion.

According to this four-linkage mechanism model and the finger joint motion ranges as depicted in Table1, the 2D workspace for one finger can be obtained, as shown in Fig. 4 (for L_1 = 45 mm, L_2 = 30 mm, L_3 = 30 mm). The other fingers workspace is similar to this one. This means that the new mechanism design should ideally cover this entire workspace.

TABLE I: FINGER JOINT MOTION RANGES (MEASURED FROM THE AUTHOR'S INDEX FINGER)

Finger Joint	Angular Motion Range (Degrees)
MCP	[-90, 60]
PIP	[-120, 10]
DIP	[-90, 30]

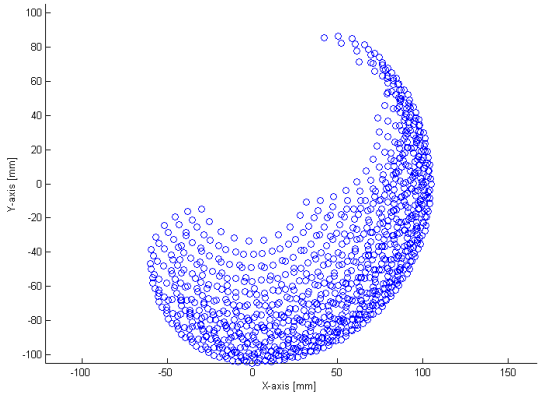

Fig. 4: Index Finger 2D Workspace

MECHANICAL DESIGN

Skeleton Design of the Mechanism

The size and shape of human fingers may vary significantly between individuals. To avoid custom design for each person, it is desirable to accommodate a large number of different people for a given design. This design requirement was accounted for by adding one additional link and degree of freedom to each finger mechanism, resulting in serial redundant link mechanisms. The haptic device mechanical skeleton is shown in Fig.5.

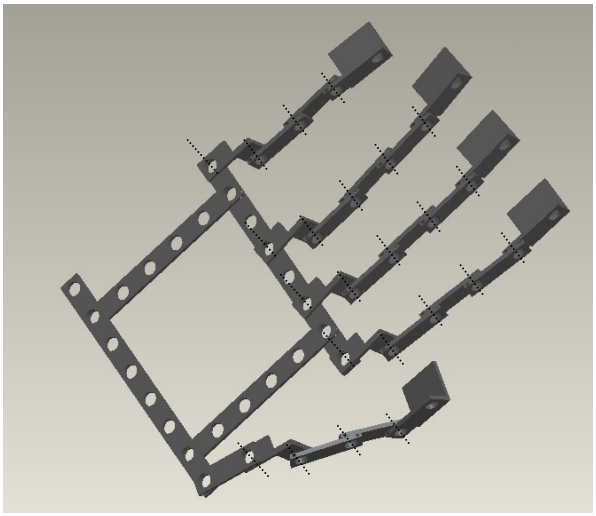

Fig. 5: CAD Model of RML-Glove Skeleton

All the joints in the design were realized through revolute pin connections. The movement of extension/flexion and adduction/abduction (which is shown in Fig.6) is possible with this mechanism. The whole mechanism is about 30 grams (without rivets). With the addition of the five linear actuators, the total weight is estimated at 105grams.

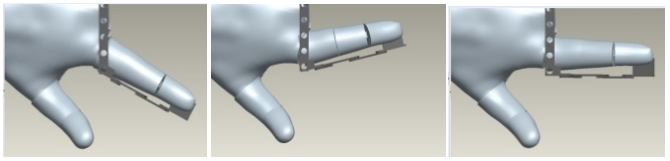

Fig. 6: Adduction and Abduction Movements

Cable Drive Mechanism

The relatively large workspace of cable-driven mechanisms is an indisputable asset for haptics. They are less costly than parallel mechanisms with rigid members; they are usually of simple design and are easily reconfigurable by changing the connection positions.

To simulate the cable in ProEngineer CAD Software, two slider mechanisms were designed on each finger to animate the cable's length change while the hand opens and closes. Fig.7 shows these results with two alternating links hidden. To make it easy to check that the 'cable' length is different while the hand is in different configurations, the sliders were assigned different colors (red and green).

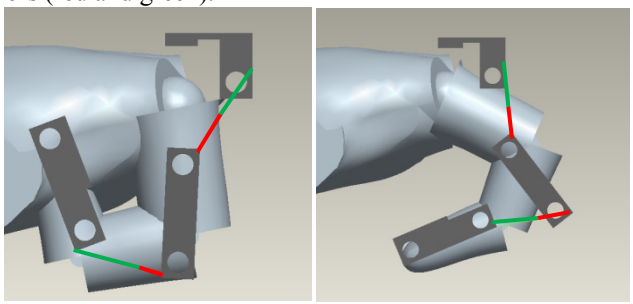

Fig. 7: Illustrations Showing the Changing Length of the Cable According to Changing Position of the Finger

KINEMATIC ANALYSES

Cabel-Drivern Mechanism Analysis

For each finger, the haptic mechanism including the finger itself constitutes a six-bar mechanism, which is shown in Fig.8. If the palm is taken as the ground part, each finger has three links, while the haptic mechanism for each finger has four links. It should be noted that the end link of the mechanism is attached to the finger tip, so they could be considered as one link. Therefore, we have 7 links in total (ground + 3 finger links + 3 haptic links) and seven revolute pin connections (ignoring the Adduction/Abduction). According to Gruebler's formula, this results in a 4 DOF mechanism for each finger.

$$F = 3(n-1) - 2f_1 - f_2 = 3(7-1) - 2 \cdot 7 = 4 \quad (1)$$

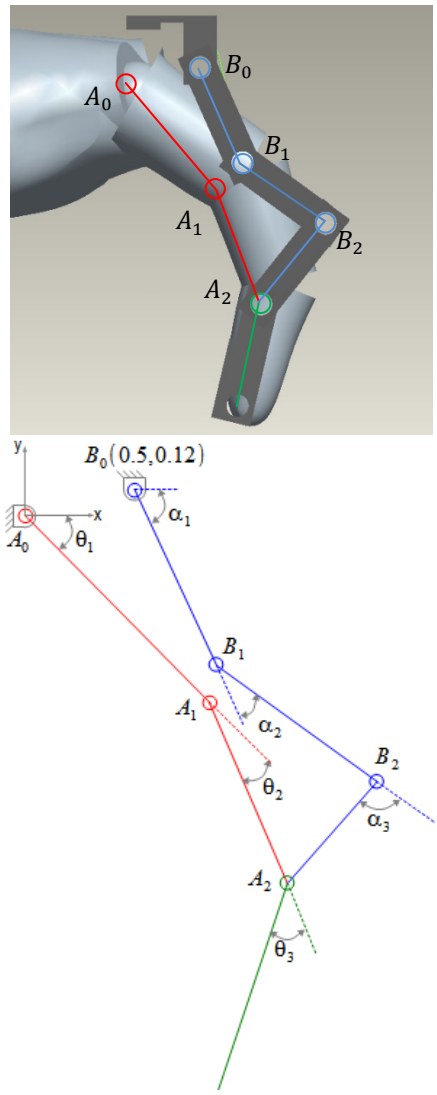

Fig.8: Six-Bar Mechanism Analysis

In order to solve the inverse kinematics of each finger mechanism, it is desired to calculate the angles for $\alpha_1, \alpha_2, \alpha_3$ from the known values of $\theta_1, \theta_2, \theta_3$. Apparently, there is more than one solution. Therefore, one additional constraint is imposed to the mechanism, which involves fixing α_2 to 30 degrees (this value was chosen based on maximizing the cable length variation.).

Based on Fig.8, the following equations can be derived:

$$0.5 + l\cos\alpha_1 + l\cos(\alpha_1+\alpha_2) + l\cos(\alpha_1+\alpha_2+\alpha_3) = \overline{A_0A_1}\cos\theta_1 + \overline{A_1A_2}\cos(\theta_1+\theta_2) \quad (2)$$

$$0.12 - l\sin\alpha_1 - l\sin(\alpha_1+\alpha_2) - l\sin(\alpha_1+\alpha_2+\alpha_3) = -\overline{A_0A_1}\sin\theta_1 - \overline{A_1A_2}\sin(\theta_1+\theta_2) \quad (3)$$

where $l = B_0B_1 = B_1B_2 = B_2A_2$

After equations (2) and (3) are solved, the angles α_1 and α_3 are plotted with respect to time using both Matlab and Pro/Engineer. It can be seen from Figs. 9 and 10 that they match very closely. This demonstrates that the simulations are correct. There are some small errors because the positions of points B_0 and A_2 are approximately measured.

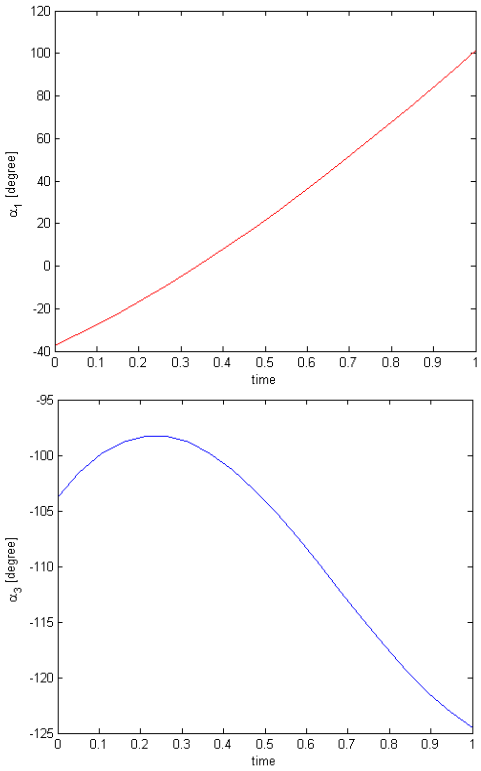

Fig. 9: Matlab Simulation for Six-Bar Mechanism

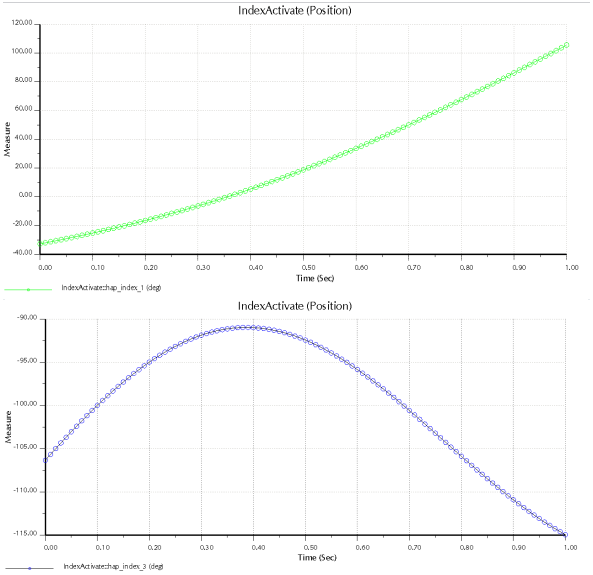

Fig. 10: Pro/E Simulation for Six-Bar Mechanism

Cable Length Analysis

Fig.11 shows the cable length analysis on the index finger. l and d are constants.

Based on Fig.11, the following equations can be derived:

$$ {}^{M}P_{N} = \begin{bmatrix} c_4 & -s_4 & 0 & l \\ s_4 & c_4 & 0 & 0 \\ 0 & 0 & 1 & 0 \\ 0 & 0 & 0 & 1 \end{bmatrix} \begin{bmatrix} c_3 & -s_3 & 0 & l \\ s_3 & c_3 & 0 & 0 \\ 0 & 0 & 1 & 0 \\ 0 & 0 & 0 & 1 \end{bmatrix} \begin{bmatrix} -d/2 \\ d/2 \\ 0 \\ 1 \end{bmatrix} $$

$$ = \begin{bmatrix} -\frac{d}{2}(c_{34} + s_{34}) \\ \frac{d}{2}(-s_{34} + c_{34}) \\ 0 \\ 1 \end{bmatrix} \quad (4) $$

$$ l_2 = \sqrt{(N_x - M_x)^2 + (N_y - M_y)^2} \quad (5) $$

From these equations, the cable length can be plotted when θ_3 and θ_4 are changing, as shown in Figs. 12 and 13. From these fingers, it can be concluded that the cable length changes are almost linear with respect to the angle changes.

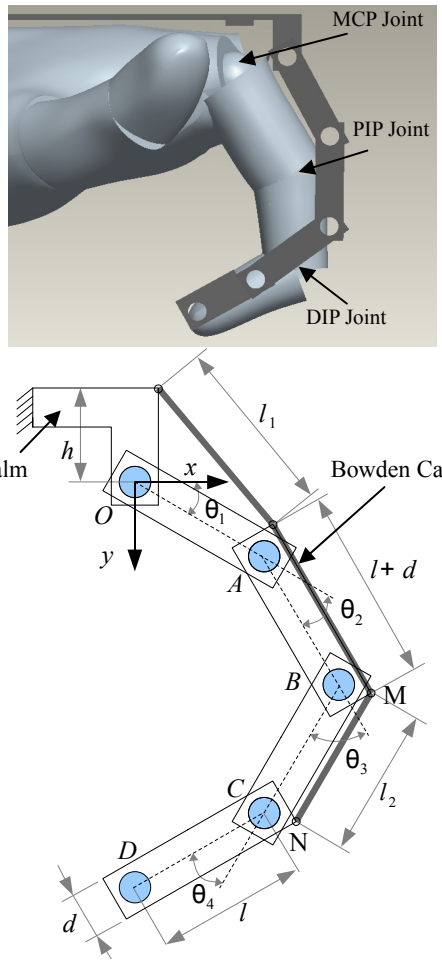

Fig. 11: Position Variables and finger kinematics model

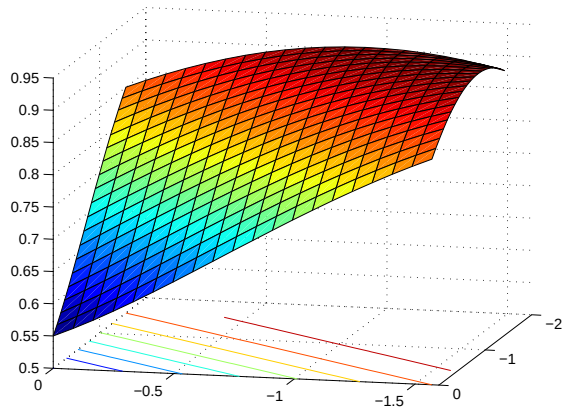

Fig. 12: Cable length vs. two joints angles (θ_3 and θ_4)

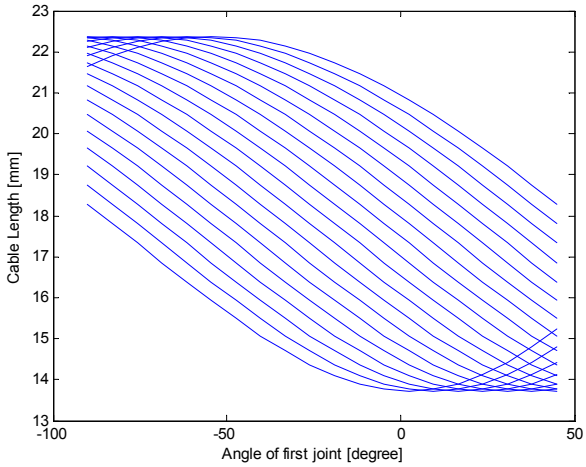

Fig. 13: Cable length vs. one joint angle (θ_3)

ELECTRICAL SYSTEM DESIGN

Force Model

This device is based on admittance measurement, which means that the input to the system is force that is measured by a force sensor, and the output is position control.

Based on several simple experiments performed, the maximum speed of movement of human fingers was estimated at about 500 mm/s (0.2s from a fist to totally open status). The strength of the thumb/finger was measured to be about 60N (based on momentary hold).

For Lead screw with high reduction (with no additional gear at the output), the maximum speed is about 0.225m/s (the motor parameters are 30000r/min@6V and 120 mA free-run), and the pitch of thread is 1.5mm. This is fast enough to follow the figures movement.

For the ball screw mechanism, the following equation describes the torque:

$$ T = \frac{Fl}{2\pi\upsilon} \quad (6) $$

where the torque T is applied to the screw or nut, F is the linear force applied, l is ball screw lead, and υ is ball screw efficiency.

With the motor's stall torque T being 20N-mm (with gear ratio of 50) and $l = 2.3mm$, the maximum force can be obtained

$$F = \frac{2\pi\upsilon T}{l} = 40N \quad (7)$$

To conclude, it was found that the RML glove is as fast as the movement of the human's fingers. The proposed device has the potential to present users with a real feel of grasp, applicable to all segments of each finger.

The Force Sensing Resistors or FSRs on the RML-Glove are robust polymer thick film devices that exhibit a decrease in resistance with increase in force applied to the surface of the sensor. They are of high performance but low cost. The force sensitivity is optimized for use for human touch control and the actuation force is as low as 0.1N and sensitivity range of 10N (maximum force can be modified in custom sensors).

Control system

The RML glove features a lead-screw structure and micro-motors dedicated to provide high-performance force-feedback. A haptic device has been described that provides a user with a realistic feeling of touch and grasp, and that are applicable to all fingers and the palm.

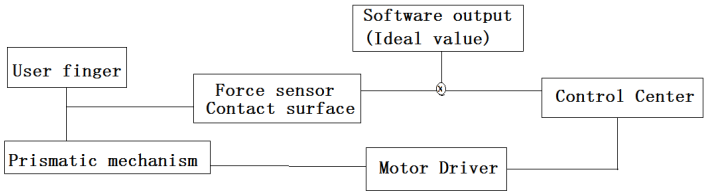

Fig. 14: Control system structure

Stability and performance are both addressed directly when impedance control is used for controller design. Impedance control regulates the behavior of the robot at the point where it interacts with the environment. Mechanical impedance is a property of the robot alone, regardless of the environment. Proper selection and ideal implementation of impedance can guarantee stability with certain environments, as well as desired feel. For example, a programmer could specify a "virtual" spring connecting the patient's hand to a position that moved along a nominal trajectory. When the patient's motion is close to nominal, the robot exerts little force. Conversely, when the patient's hand strays, the robot pushes or pulls it back to the nominal motion; the farther the patient strays, the greater the force the robot exerts.

Wireless communication with robot or host PC is operated in unlicensed bands of 2.4 GHz. The interface consists of micro-motors, force sensitive sensors, lithium-ion battery, wireless RF module, and an ARM7 micro-controller board. The onboard CPU monitors velocity in real time and enables electromagnetic damping on the haptic device if a problem occurs on the host computer.

CONCLUSION

A haptic device has been described that provides a user with a realistic feeling of touch and grasp, and that is applicable to all fingers and the palm, as opposed to being applicable to the finger tips only. The haptic devices described in comparison may be capable of responding to gesture signals at relatively high frequencies, thereby providing an extremely realistic and dynamic sense of grasp. These haptic devices may have maximum number of pressure points for force feedback, and hence may provide force feedback to a large number of relevant pressure points, up to about fifteen. No unrealistic or unnecessary force may be exerted on unwanted areas on the fingers. Force feedback may be bidirectional, i.e., force may be applied both under and above each finger segment. Also, the force feedback mechanism may be engaged at the hand area rather than at remote cable-connected locations that generally result in a sluggish and unrealistic sense of grasp, because of cable stretch and accumulation of various mechanical backlashes. These haptic devices may perform gesture measurements without need for additional devices such as exoskeleton gloves, and therefore may be worn on the bare hand with minimal intrusive hardware. Finally, these haptic devices may potentially be manufactured at a relatively low cost.

ACKNOWLEDGMENTS

The authors would like to thank Mathieu Barraja and Chad Gilman for the fruitful discussions, and William Rutkowski for the manufacture of the prototype of the device.

REFERENCES

[1] C. Basdogan, C. H. Ho, and M. A. Srinivasan, "Virtual environments for medical training: Graphical and haptic simulation of laparoscopic common bile duct exploration," IEEE/ASME Trans. Mechatron., vol.6,no. 3, pp. 269–286, Sep. 2001.

[2] A. Bardorfer, M.Munih, A. Zupan, and A. Primozic, "Upper limb motion analysis using haptic interface," IEEE/ASME Trans. Mechatron.,vol.6, no. 3, pp. 253–260, Sep. 2001.

[3] N. A. Langrana, G. Burdea, K. Lange, D. Gomez, and S. Deshpande, "Dynamic force feedback in a virtual knee palpation," Artif. Intell. Med., vol. 6, pp. 321–333, 1994.

[4] I. Ivanisevic and V. J. Lumelsky, "Configuration space as a means for augmenting human performance in teleoperation tasks," IEEE Trans. Syst., Man Cybern. B, vol. 30, no. 3, pp. 471–484, Jun. 2000.

[5] R. V. Dubey, S. E. Everett, N. Pernalete, and K. A. Manocha, "Teleoperation assistance through variable velocity mapping," IEEE Trans. Robot.

[6] I. Elhajj, N. Xi, W. K. Fung, Y. H. Liu, W. J. Li, T. Kaga, and T. Fukuda, "Haptic information in internet-based

teleoperation," IEEE/ASME Trans. Mechatron., vol. 6, no. 3, pp. 295–304, Sep. 2001. Autom., vol. 17, no. 5, pp. 761–766, Oct. 2001.
[7] N. Ando, P. Korondi, and H. Hashimoto, "Development of micromanipulator and haptic interface for networked micromanipulation," IEEE/ASME Trans. Mechatron., vol. 6, no. 4, pp. 417–427, Dec. 2001.
[8] O. D. Gabriel Sepulveda, Vicente Parra. "Haptic cues for effective learning in 3d maze navigation", IEEE International Workshop on Haptic Audio Visual Environments and Games, Ottawa.Canada, October 2008.
[9] M. Guthold, M. R. Falvo, W. G. Matthews, S. Paulson, S. Washburn, D.A. Erie, R. Superfine, F. P. Brooks, Jr., and R.M. Tylor, "Controlled manipulation of molecular samles with the nanomanipulator," IEEE/ASME Trans. Mechatron., vol. 5, no. 2, pp. 189–198, Jun. 2000
[10] S. Marliere, D. Urma, J. Florens, and F. Marchi, "Mult-sensorial interaction with a nano-scale phenomenon: The force curve," in Proc. EuroHaptics, 2004, pp. 246–252.
[11] V. Hayward, and K.E. Maclean, "Do it yourself haptics: part I " Robotics & Automation Magazine, IEEE Vol. 14 , no. 4, pp. 88-104, 2007.
[12] D. A. Norman, "The next UI breakthrough, Part 2: Physicality,'' ACM Interact., vol. 14, no. 3, pp. 44–45, 2007.
[13] Hayward, V. and Maclean, K.E., "Do it yourself haptics: part II [Tutorial] ", Robotics & Automation Magazine, IEEE Vol. 15 , no. 1, pp. 104-119, 2008.
[14] K. E. MacLean, ''Haptics in the wild: Interaction design for everyday interfaces,'' Reviews of Human Factors and Ergonomics, M. Carswell, Ed.Santa Monica, CA: Human Factors and Ergonomics Society, to be published
[15] R. V. Dubey, S. E. Everett, N. Pernalete, and K. A. Manocha, "Teleoperation assistance through variable velocity mapping," IEEE Trans. Robot. Autom., vol. 17, no. 5, pp. 761–766, Oct. 2001.
[16] I. Elhajj, N. Xi, W. K. Fung, Y. H. Liu, W. J. Li, T. Kaga, and T. Fukuda," Haptic information in internet based teleoperation," IEEE/ASME Trans. Mechatron., vol. 6, no. 3, pp. 295–304, Sep. 2001.
[17] Immersion Corporation. CyberGlove, Available online: http://www.immersion.com.
[18] Mourad Bouzit, Grigore Burdea, George Popescu, and Rares Boian. "The Rutgers master II - new design force feedback glove," IEEE/ASME Transactions on Mechatronics, vol 7, no. 2, pp. 256-263, 2002.